

Seventh Framework Programme

Theme 6

Environment



Project: 603864 – HELIX

Full project title:

High-End cLimate Impacts and eXtremes

Deliverable: 3.3

The impact of Arctic SST/SIC changes and North Atlantic Ocean SST changes associated with high end SWLs on European climate variability

Version 1.0



Original Due date of deliverable: 30/04/17

Actual date of submission:

**The impact of Arctic SST/SIC
changes and North Atlantic
Ocean SST changes associated
with high end SWLs on
European climate variability
Deliverable Title**

April

2017

Executive Summary

The IPCC AR4 (2013) concluded that global warming has more profound impacts in the polar region. The Arctic is warming nearly twice as fast as the global average; a phenomenon referred to as Arctic amplification. An analysis of observations suggests a robust linkage between the Arctic and mid-latitudes. However, many models simulate only a weak and often ambiguous connection. The response of mid-latitude weather and climate to Arctic sea ice loss is not well-understood, particularly in a future warmer climate. This report focuses on the response of regional variability to the variation of Arctic sea ice extent in a 4 degree warmer world (SWL4).

For this report AMIP-style EC-EARTH model integrations have been performed to study the local and remote response to Arctic sea ice variation. The results indicate that the atmospheric response is not restricted to the Arctic region, with impacts also in found in remote regions. Both the inter-annual variability of sea ice and the magnitude of sea ice loss play a critical role in influencing European weather and climate.

For surface air temperature (SAT), the response to a sea ice variation shows a large spread compared to the reference EC-EARTH SWL4 run. In spring, the magnitude of sea ice loss has more profound local warming/cooling effects, with robust changes occurring mainly in the Arctic region. Less robust warmer SAT remote response is seen over Eastern Europe under low sea ice condition. Accounting for sea ice inter-annual variability we find a weakly warmer SAT. In summer, low sea ice condition (ice-free Arctic) leads to a robust warm SAT response over central Europe. In autumn, the most profound warming is found over central Eurasia from the sea ice inter-annual variability experiment. Both high and low sea ice conditions lead to small regions with significantly different SAT in central Europe. In winter, both high and low sea ice conditions show a strong cooling over central Europe.

Notable impacts on precipitation from sea ice inter-annual variability are found in autumn over high-latitude ocean areas and in spring over mid-latitude land regions. The response to the magnitude of sea ice loss is only robust in December to April over the high-latitude ocean region. The spatial distribution of precipitation in all sensitivity experiments reveals only minor differences over Europe. Stronger local responses of P-E (precipitation minus evaporation) occur over Arctic in spring and winter, and occasional robust remote responses are found in the western Pacific Ocean depending on the season. Significant changes in runoff are only found in Arctic coastal region of the northern continents in spring and summer. Salient snow depth variations are found in northern Canada and Eurasia in winter and spring.

Possible changes in the frequency of occurrence of extreme events are studied with a blocking frequency analysis. Robust changes in the blocking frequency are found in winter that can be associated with sea ice inter-annual variability. On the other hand, the magnitude of sea ice loss has no clearly discernible impact on the winter blocking frequency. The experiments with either higher or lower sea ice extent show both a similarly increased blocking frequency over Europe. In spring, high sea ice condition lead to significant increasing of blocking frequency. In autumn, a decrease in the blocking frequency over Europe is found with both high and low sea ice extent experiments.

The circulation response due to sea ice loss and natural variability plays a critical role in modulating atmospheric local and remote response. The most robust changes occur in winter and spring, when a strong sea ice loss results in a weaker and slowly eastward moving jet stream which contributes to more cold weather over Central Eurasia.

The impact of Arctic SST/SIC changes and North Atlantic Ocean SST changes associated with high end SWLs on European climate variability

Shiyu Wang, Klaus Wyser, Gustav Strandberg

1. Introduction

In the past few decades, profound changes have been occurred in the Arctic. Rapid Arctic sea ice decline has been observed since at least 1979; particularly the September sea ice cover has declined by 40% (e.g. Screen, 2017). Observation shows that the Arctic is warming nearly twice as much as the global average. This phenomenon is termed the Arctic amplification and has occurred over all seasons, yet particularly pronounced in autumn and winter. The Arctic warming has triggered significant local and remote impacts on weather and climate, which has received a lot of scientific attentions (e.g. Barnes, 2013; Screen, 2013a, 2013b, 2014 and 2017). There is emerging evidence that the Arctic sea ice loss has possible linkages with extremes and large-scale circulation variability over Europe. Mori et al. (2014) found that sea ice decline leads to more frequent Eurasian blocking, hence in turn has favoured more severe winters in past decades. Observational evidence shows that this is more likely associated with the negative phase of the North Atlantic Oscillation (NAO) (Honda, 2009). Screen (2013a) suggests a causal link that diminishing Arctic sea ice may has contributed to the increased summer rainfall over northern Europe. In addition to associated mid- and high-latitude impacts, large uncertainty also arises for low-latitude impacts, Screen et al. (2015) found that the likelihood and severity of wet extremes over the Mediterranean are increased in climate projections as a consequence of Arctic sea ice loss. However, a physical linkage between Arctic sea ice decline and European climate remains unclear. Screen (2017) found that the Arctic sea ice loss does not lead to Northern European winter cooling due to a strong thermodynamical effect. Most model simulations show that the atmospheric response is highly non-linear and small compared with the atmospheric internal variability (e.g. Barnes, 2015; Petrie, 2015; Screen, 2014).

Under a warming climate, it is very likely that the Arctic sea ice cover will continue shrinking and the September Arctic sea ice could nearly disappear by the end of 21st century under a high emission scenario (IPCC, 2013). The CMIP5 (5th phase of the Coupled Model Intercomparison Project) multi-model projections show a large variability among different climate models in the magnitude and severity of Arctic sea ice loss. Some models are very conservative in simulating Arctic sea ice loss, while others show a more rapid and severe decline. Given the complexity and non-linearity of physical feedbacks, it is unclear how the atmosphere responds to these differences in the sea ice forcing. It is plausible that the atmospheric response may be quite different in warmer climate depending on the amount of the Arctic sea ice that is left. The aim of this study is to address and understand the risk of large changes and the sensitivity to extreme Arctic sea ice extent changes at a 4°C specific warming levels (SWL4),

2. Methodology and experiment setup

To investigate the potential climate response to an extreme Arctic sea ice decline in a warmer climate, we have selected to study the sensitivity to Arctic sea ice in SWL4 which is a 4 degrees warmer climate relative to pre-industrial level (Gohar et al. 2014). We first studied the range of Arctic sea ice representations in the CMIP5 models and selected one model that retains a lot of sea ice in the Arctic summer at the end of the 21st century for the HI-ICE experiment. Similarly we were looking for a CMIP5 model with little sea ice to span the full range but couldn't find a suitable model that would reach an almost ice-free Arctic even during winter before the end of the 21st century. Thus, we looked further into the future and picked a CMIP5 model with no summer sea ice in summer and little seasonal sea ice cover in winter in the 2nd half of the 22nd century. The details of the selected CMIP5 models and timeslices used for the forcing are listed in Table 1.

The sensitivity study is done with the EC-EARTH 3.1 model with T255 spectral truncation (corresponds to ~80 km resolution) and 91 vertical levels (Alfieri et al, 2017). The atmosphere-only model (AMIP style) is forced with prescribed SST and sea ice concentration (SIC) at the lower boundary. The EC-Earth model¹ in the CMIP5 database reaches SWL4 in 2083. We take the average annual cycle of SST from the CMIP5 EC-Earth model and use it as a climatological SST forcing for all experiments. Four different SIC forcings have been prepared for the sensitivity study:

1. Climatological SIC annual cycle from CMIP5 EC-Earth similar to the climatological SST
2. The full timeseries of SIC for 2080-2090 from CMIP5 EC-Earth
3. Climatological SIC annual cycle from CMIP5 CNRM-CM5 averaged during 2078-2098
4. Climatological SIC annual cycle from CMIP5 CNRM-CM5 averaged during 2160-2180

Further details to the SST and SIC forcings are given in Table 1. Each sensitivity experiment comprises 10 ensemble members of 11-year of integration, resulting in a total sample size of 110 model years per experiment for the statistical evaluation. Each ensemble member starts from a slightly different initial state to allow us to study the natural variability. The GHG (Greenhouse Gas), aerosol and ozone forcing in all experiments is for years 2080-2090 of RCP8.5 which corresponds to SWL4 for the CMIP5 EC- Earth model.

The prescribed annual cycle of SIC averaged over North Hemisphere for REF, HI-ICE and LO-ICE experiments are shown in Figure 1. The reference EC-Earth SWL4 run (REF) and the CNRM-CM5 SWL4 (HI-ICE) run have similar temporal variation, except that HI-ICE experiment shows more sea ice from February to June and less sea ice from July to next January compared to the REF experiment. LO-ICE is the extreme scenario with an almost complete loss of Arctic sea ice: the sea ice completely disappears from June to December and only minor sea ice extent from January to May. To investigate the impact of inter-annual variability of sea ice, the actual sea ice cover from the EC-Earth SWL4 period are used as forcing fields in the IAV experiment. Apart from assessing the sensitivity to inter-annual variability the difference between REF and IAV also allows us to judge the representativeness of our other experiments that were built on climatological SIC forcing.

¹ The scenario simulations for CMIP5 were done with an older version (2.3) of the EC-Earth model and with lower resolution (T159).

Table 1: Summary of the sensitivity experiments setup

| Experiment | SST forcing | SIC forcing | Ensemble size | Analysis period | Remark |
|------------|---|---|---------------|----------------------|--------------------------------|
| REF | Climatological annual cycle from the CMIP5 EC-Earth at SWL4 (years 2073-2093 with the RCP85 scenario) | Climatological annual cycle from the CMIP5 EC-Earth at SWL4 | 10 | 11 consecutive years | Reference |
| IAV | as REF | Real SIC (year-to-year variation) from the CMIP5 EC-Earth simulation during years 2080-2090 (with the RCP85 scenario) | 10 | 11 consecutive years | Inter-annual variability |
| HI-ICE | as REF | Climatological annual cycle from CMIP5 CNRM-CM5 at SWL4 (2078-2098 with the RCP85 scenario) | 10 | 11 consecutive years | High amount of sea ice at SWL4 |
| LO-ICE | as REF | Climatological annual cycle from CMIP5 CNRM-CM5 for a late period (2160-2180, extended RCP85 scenario) | 10 | 11 consecutive years | Low amount of sea ice |

3 Results

3.1 Climate response over Eurasia

The Arctic sea ice loss plays a critical role for weather and climate, both locally and remotely. The largest local effect is the reduced surface albedo that alters heat and moisture fluxes between the atmosphere and ocean. The atmospheric response strongly depends on seasons and regions. Figure 2 shows the annual cycle of precipitation averaged over land and ocean in high- and mid-latitude regions. The differences between different experiments are found to be small in high- and mid-latitudes over land. During spring, precipitation is found to be larger in the IAV experiment over mid-latitude land region which indicates that the sea ice inter-annual variation has much larger contribution to precipitation response in mid-latitude land area than the magnitude of sea ice loss. A similar pattern is also seen in the high-latitude ocean region in fall. However, the most striking impacts are seen during winter over high-latitude ocean regions in the case of strong sea ice reduction (LO-ICE).

Figure 3 illustrates the annual cycle of surface air temperature (SAT). The SAT response to sea ice inter-annual variability (IAV) has the same seasonal variation in both high- and mid-latitude land and ocean regions compared to the REF experiment. Substantial SAT differences are caused by large and systematic sea ice variations represented by HI-ICE and LO-ICE. From January to April, the large Arctic sea ice variation has led to a robust warming or cooling

in high-latitude ocean regions and from May to June the SAT differences between the HI-ICE and LO-ICE experiments are much smaller (Figure 3), despite the still large sea ice extent difference (Figure 1). A similar response is also detected over high-latitude land areas, but the magnitude of cooling and warming is much smaller than over the ocean.

To further investigate the spatial distribution of atmosphere response, Figure 4 shows the SAT differences between the reference run (REF) and the other experiments in spring (MAM) and winter (DJF). During spring, the differences between IAV and REF show wide a spread warm bias over Eurasia except minor cooling adjacent to the Mediterranean Sea, in particularly the warming in southern Europe is quite pronounced. The differences between HI-ICE and REF experiments show a substantial cold bias over large parts of Europe, especially in the Arctic region. Vice versa, the low sea ice experiment (LO-ICE) leads to a large warm bias over the Arctic that also extends to central Europe compared to REF. In winter, the IAV experiment exhibits a cold bias in the Arctic and a small warm bias in southern Europe with a weaker cold bias over central Europe. Similar to the situation in spring, the high sea ice experiment (HI-ICE) shows strong cooling over the Arctic and central Europe, except for a strong warming in the Beaufort-Chukchi Sea and Hudson-Baffin Bay which could be due to spatial distribution of sea ice. The spatial distribution of the differences between LO-ICE and REF are characterized by the warm Arctic-cold continents pattern, which is similar to the results of Mori et al. (2014). As discussed in Mori et al. (2014), this pattern is associated with a positive contribution to the cooling of Eurasia. However, a positive Arctic Oscillation trend could weaken the cooling effect and further decrease the frequency of cold winters. During summer, central Europe exhibits a significant warming under low sea ice condition (ice-free Arctic). Sea ice inter-annual variability experiment also shows a warming over whole Europe, but only significant in some patches over northern Europe, and the magnitude is much smaller (not shown). In autumn, the most profound warming is found in central of Eurasia when comparing IAV and REF. Both HI-ICE and LO-ICE lead to minor patches of regional warming in central Europe(not shown).

Based on observational data the Arctic warming associated with sea ice loss may favour the occurrence of cold winter extremes at middle latitudes of the northern continents (Tang, 2013). As an example the Stockholm region had its snowiest November day in 2016 since 1905 which lead to a widespread public transportation chaos. To assess the potential for changes in extremes we analyse the seasonal blocking frequency (Figure 5). The definition for blocking is adopted from Trigo et al. (2004). In winter (DJF), all experiments lead to similar numbers of blocking events over Eastern Eurasia between 30°E-90°E except for LO-ICE in which we find slightly more blocking events. Over central Europe between 0-30°E all experiments show more blocking events compared to the REF experiment. In both high and low sea ice experiments (HI-ICE and LO-ICE) we find similar blocking frequencies which indicates that blocking in winter over Europe is not sensitive to the severity of sea ice loss. On the other hand, the sea ice inter-annual variability (IAV) shows a more robust change in blocking frequency compared to the REF experiment. The more frequent occurrence of cold winters associated with Arctic sea ice loss may be a temporary phenomenon, albeit more cold winters have been observed recently (Mori et al., 2014). In spring (MAM), the largest response in blocking events over central Europe is associated with HI-ICE. In summer (JJA), LO-ICE shows a tendency for more blocking over central Europe (0-30°E) compared to HI-ICE. In autumn (SON), HI-ICE and LO-ICE show reduced blocking frequency compared to the REF experiment. Furthermore, over central Europe LO-ICE also leads to more frequent blocking..

3.2 Climate response to the magnitude of sea ice loss

From the variability of the results we conclude that climate projections still have large uncertainties that at least to some extent are due to inter-annual variability of Arctic sea ice. The relative importance of the inter-annual variability

and the magnitude of sea ice loss is still unclear. In order to help with the interpretation of the impacts that can be attributed to the magnitude of the sea ice loss, we now focus on the comparison between high (HI-ICE) and low sea ice (LO-ICE) experiments.

Figure 6 shows the seasonal precipitation differences between LO-ICE and HI-ICE. In spring and winter, LO-ICE has simulated more precipitation over central of Arctic and less precipitation in the south and east side of Greenland. Away from the Arctic, the precipitation differences over Eurasia are rather small in all seasons, in agreement with the results shown in Figure 2. The precipitation response is strengthened by the moisture availability due to surface warming.

The Arctic warming has been found to increase the downward infrared radiation mainly linked to an increased cloud cover (Francis, 2007). The total cloud cover (TCC) responses are shown in Figure 7. Due to the local feedback mechanism, substantial differences in TCC are found in the vicinity of the Arctic in spring and winter. TCC is higher in HI-ICE over majority of the Arctic, except over the Kara Sea and Beaufort Sea in spring where LO-ICE has more clouds. Small patches with reduced cloud cover are also found in central of Eurasia in spring and east of Europe in summer.

Precipitation minus evaporation (P-E) differences are illustrated in Figure 8. Robust differences are found over the Arctic region in winter and spring. Considering the large sea ice difference in these seasons, the increased air temperature in LO-ICE due to increased absorption of solar radiation leads to stronger evaporation. In sea ice free seasons (summer and autumn), striking differences are found in the West Pacific Ocean. The difference in P-E between LO-ICE and HI-ICE are found to be small over northern continents in all the seasons.

Figure 9 shows the runoff differences between LO-ICE and HI-ICE experiments. Minor differences are barely noticeable over Eurasian in autumn and winter. In spring and summer pronounced response mainly occurred in northern Canada and the Siberian coast region. Interestingly we also find a remote response in the runoff in Southeast Asia in summer and autumn.

The response of the snow cover extent to the variation of the Arctic sea ice is not significantly different, both LO-ICE and HI-ICE produce similar seasonal variation (figure not shown). However, we find significant changes in the snow depth in winter and spring. In winter LO-ICE shows reduced snow depth compared to HI-ICE in eastern Eurasia and slightly increased snow depth over western Siberia. The largest differences are found adjacent to the Bering Strait. North America also experiences deeper snow pack under the LO-ICE scenario. In spring, we find a similar pattern of the snow depth distribution over Eurasia, but the magnitude is much stronger in LO-ICE. However, snow depth is largely reduced over large part of northern Canada in LO-ICE.

A more robust response to the variation of Arctic sea-ice is found for SAT (Figure 11). Strong warming is mainly found in the Arctic and adjacent regions in response to large sea ice loss, including Canada and Western Siberian. In spring, this robust signal further extends into Eastern Europe, while strong cooling is found over southern Eurasia. A similar pattern is also found in winter, but the cooling is much weaker. However, the extreme warming around Greenland could increase the probability of passing the tipping point for melting of the Greenland Ice sheet (Kriegler, 2009). In

summer, LI-ICE results in a significant warming over central Europe, Western Siberian and northern Canada. In autumn, small patches of warming occur in the vicinity of Greenland. One of the main features of declining sea ice are the altered fluxes between atmosphere and ocean. Reduced sea ice cover leads to lower surface albedo and stronger absorption of solar radiation by the open water, yet at the same time the ocean surface is warmer than the sea ice which results in a larger heat transfer from the ocean to the atmosphere. Figure 12 illustrates the seasonal turbulence fluxes (sensible + latent heat fluxes) response due to sea ice loss. Strong increases are found adjacent sea ice loss region in spring and winter. The altered turbulent fluxes further affect the air temperature (Figure 11) and moisture, as well as the formation of clouds (Figure 7).

The remote responses over high and mid-latitude regions are much more complicated and strongly modulated by large circulation changes. All our experiments are characterized by extremely low sea ice cover in autumn compared to present-day conditions (Figure 1). The anomalous low sea ice extent could lead to a negative North Atlantic Oscillation (NAO) /Arctic Oscillation (AO) pattern in the following winter (Liu, 2012). To elucidate the impact of Arctic sea ice decline on the atmospheric circulation, the SLP response between the low (LO-ICE) and high sea ice (HI-ICE) experiments are shown in Figure 13. A positive SLP anomaly is found over Greenland in winter and spring. In winter, there is cyclonic SLP anomaly over the central Arctic region and anticyclonic SLP anomaly over the North Pacific which indicates a weaker Aleutian low. A slightly intensified Siberian High is also represented by a positive SLP anomaly over Eurasian continent (Mori, 2014), leading to cold advection and more frequent occurrences of cold air outbreaks over eastern Eurasia (Takaya, 2005). Similarly, much larger positive SLP anomaly is found in spring, which also leads to more cold events in eastern Eurasia (Figure 11).

Figure 14 shows the geopotential height response at 500hPa. The geopotential is found to be higher over the Arctic in winter (DJF) and spring (MAM) in LO-ICE. Less sea ice also causes a decrease in geopotential height from mid-Atlantic to Western Europe. It is notable that this pattern is strongly coherent with a negative phase of NAO, consistent with a robust Arctic surface warming in winter and spring (Figure 8). To further investigate the 1000-500hPa layer thickness variation due to a warm surface temperature anomaly, global zonal mean geopotential height vertical profiles are calculated. Figure 15 illustrates that the north-south gradient of 1000-500hPa layer thickness are lower in LO-ICE in all seasons, particularly in MAM and DJF, which according to the thermal wind law correspond to a lower the mid tropospheric zonal wind speed (Vihma, 2014).

Figure 16 shows the 300hPa zonal wind response (U300). It depicts strong seasonal variability and large variability in the geographical pattern. In winter, HI-ICE has lower U300 over central Europe yet higher U300 over the mid-Atlantic. In spring, the U300 differences between LO-ICE and HI-ICE over North Atlantic-Europe are reversed and the magnitude is larger. Both patterns tend to favour a weaker jet stream in LO-ICE which allows the cold polar air to penetrate further south. The overall vertical global zonal mean wind response also shows that the sea ice loss results in weaker westerlies which push the cold Arctic air further south into the middle latitude region and cause more cold weather in winter and spring (Figure 17).

The circulation impacts are also supported by the vertical temperature gradient in spring and winter. The north-south temperature gradient is significantly lower in HI-ICE near the surface which indicates a strong equatorward shift of the jet stream, while at higher altitudes the differences in the temperature gradient and the poleward shift of the jet stream are smaller. (Figure 18).

4 Summary

The aim of this report is to investigate the key regional circulations system variation and climate variability due to Arctic sea ice loss at 4°C specific warming level (SWL4). Four AMIP-style sensitivity experiments with varying sea ice cover under SWL4 conditions have been carried out.

The results show that both the sea ice inter-annual variability and magnitude of Arctic sea ice loss play a critical role for European weather and climate. However, atmospheric response due to sea ice decline is strongly seasonal and geographical regions dependent. Notable impacts from sea ice inter-annual variability on precipitation are found in autumn over high-latitude ocean areas and in spring over mid-latitude land region. The response to the magnitude of sea ice loss is only robust in December to April over the high-latitude ocean region. The spatial distribution of precipitation in all sensitivity experiments reveals only very minor differences over Europe. Stronger local responses of P-E are apparent over the Arctic in spring and winter and robust remote responses are found in the western Pacific Ocean depending on seasons. Significant changes in the continental runoff are found in the Arctic coastal region in spring and summer. All sensitivity experiments show similar seasonal variations of the snow cover extent. However, striking snow depth variations are found in northern Canada and Eurasia in winter and spring.

The impact of the variation in sea ice on the occurrence of extreme events are analysed by studying the changes in the blocking frequency. Robust changes in the blocking frequency are found during winter associated with sea ice inter-annual variability. Both high and low sea ice extent experiments show a similarly increased blocking frequency over Europe, which indicates that the winter blocking over Europe is not sensitive to the magnitude of Arctic sea ice loss. In spring, a pronounced increase of blocking events is simulated in the high sea ice experiment compared to the other experiments. In autumn, decreased blocking frequency over Europe is found with both high and low sea ice extent experiments.

For surface air temperature (SAT), the response to sea ice variations show much larger diversity. Comparing to the reference run (REF), in spring, magnitude of sea ice loss has more profound local warming/cooling effects. The most robust response is found for the Arctic region. A less robust warmer SAT remote response is seen over Eastern Europe under low sea ice condition. Accounting for the sea ice inter-annual variability induces a weaker warmer SAT. In summer, low sea ice condition (ice-free Arctic) lead to a robust warm SAT response over central Europe. In autumn, most profound warm changes are found in central Eurasia due to sea ice inter-annual variability. In winter, both high and low sea ice condition cause cooling over Europe, in particular HI-ICE conditions shows much stronger cooling.

The circulation response due to sea ice loss and sea ice inter-annual variability play a leading role in modulating atmospheric local and remote response. A significant response due to sea ice loss is seen in winter and spring. The reduced north-south gradient of 1000-500hPa layer thickness results in a reduction of the mid tropospheric zonal wind speed. According to Rossby wave theory, weakened and slowly eastwards moving jet stream results in weaker westerlies which push cold Arctic air further south into the mid-latitude region and cause more cold weather in winter and spring over eastern Eurasia. The strength of the response due to sea ice inter-annual variability needs further investigation.

Reference

- Alfieri L, Bisselink B, Dottori F, Naumann G, de Roo A, Salamon P, Wyser K and Feyen L 2017 Global projections of river flood risk in a warmer world, *Earth's Future*, doi:10.1002/2016EF000485
- Barnes, EA, 2013, Revisiting the evidence linking Arctic amplification to extreme weather in midlatitudes, *Geophys Res. Lett.*, 40:4728-4733
- Barnes, EA, Screen, JA, 2015, The impact of Arctic warming on the midlatitude jet-stream: Can it? Has it? Will it? *WIREs clim. Change*, 6:277-286. doi:10.1002/wcc.337
- Francis, J.A. and E. Hunter, 2007, Changes in the fabric of the Arctic's greenhouse blanket. *Environ. Res. Lett.* 2, doi:10.1088/1748-9326/2/4/045011
- Gohar LK, Bernie D and Lowe JA. 2014. Evaluation of timing of SWLs from existing models. Report D2.1 to the HELIX programme.
- Honda, M., Inoue, J., Yamane, S., 2009, Influences of low Arctic sea ice minima on anomalously cold Eurasian winter, *Geophys. Res. Lett.*, 36, L08707, doi:10.1029/2008GL037079
- Intergovernmental Panel on Climate Change (IPCC), 2013, The Physical Science Basis. Contribution of working group I to the fifth assessment report of the intergovernmental panel on climate change. T.F. Stocker et al., Eds, Cambridge, University Press, Cambridge, UK and New York, NY, USA, 1552p
- Kriegler, E. Jim W. Hall, Hermann Held, Richard Dawson and Hans Joachim Schellnhuber, 2009. Imprecise probability assessment of tipping points in the climate system. *Proceedings of the National Academy of Science* 106(13), 5041
- Liu, J., Curry JA, Wang H, Song M and Horton R., 2012, Impact of declining Arctic sea ice on winter snowfall. *Proc. Natl. Acad. Sci. U.S.A.* 109:4074-4079, doi:10.1073/pnas.1114910109
- Petrie, R.E., Shaffrey, L.C., Sutton, R.T. 2015, Atmospheric response in summer linked to recent Arctic sea ice loss, *Q.J.R. Meteorol. Soc.* doi:10.1002/qj.2502

Screen, J.A., 2013a, Influences of Arctic sea ice on European summer precipitation, *Environ. Res. Lett.*, 8, doi:10.1088/1748-9326/8/4/044015

Screen JA, Simmonds I., 2013b, Exploring links between Arctic amplification and mid-latitude weather, *Geophys Res. Lett.*, 40:959-964

Screen, JA, Deser, C., Simmonds, I., Tomas, R., 2014, Atmospheric impacts of Arctic-ice loss, 1979-2009: separating forced changes from atmospheric internal variability. *Clim. Dyn.* 43:333-344, doi:10.1007/s00382-013-1830-9

Screen, J.A., Deser, C., Sun, L., 2015, Projected changes in regional climate extremes arising from Arctic sea ice loss, *Environ. Res. Lett.* 10, 084006, doi:10.1088/1748-9326/10/8/084006

Screen J.A, 2017, The missing Northern European winter cooling response to Arctic sea ice loss. *Nat. Commun.* 8, 14603 doi: 10.1038/ncomms14603

Takaya, K and Nakamura, H., 2005, Geographical Dependence of Upper-Level Blocking Formation Associated with Intraseasonal Amplification of the Siberian High, *J. Atmos. Sci.*, 62, 4441-4449

Tang, Q. H., Zhang, X. J., Yang, X. H. and Francis, J. A. 2013. Cold winter extremes in northern continents linked to Arctic sea ice loss. *Environ. Res. Lett.* 8, 014036

Trigo, R.M., Trigo, I.F., DaCamara, C.C. and T. J. Osborn, 2004, Climate impact of the European winter blocking episodes from the NCEP/NCAR Reanalyses, *Climate Dynamics*, 23: 17. doi:10.1007/s00382-004-0410-4

Vihma, T., 2014, Effects of Arctic sea ice decline on weather and climate: A review, *Surv. Geophys.* 35:1175-1214, doi:10.1007/s10712-014-9284-0

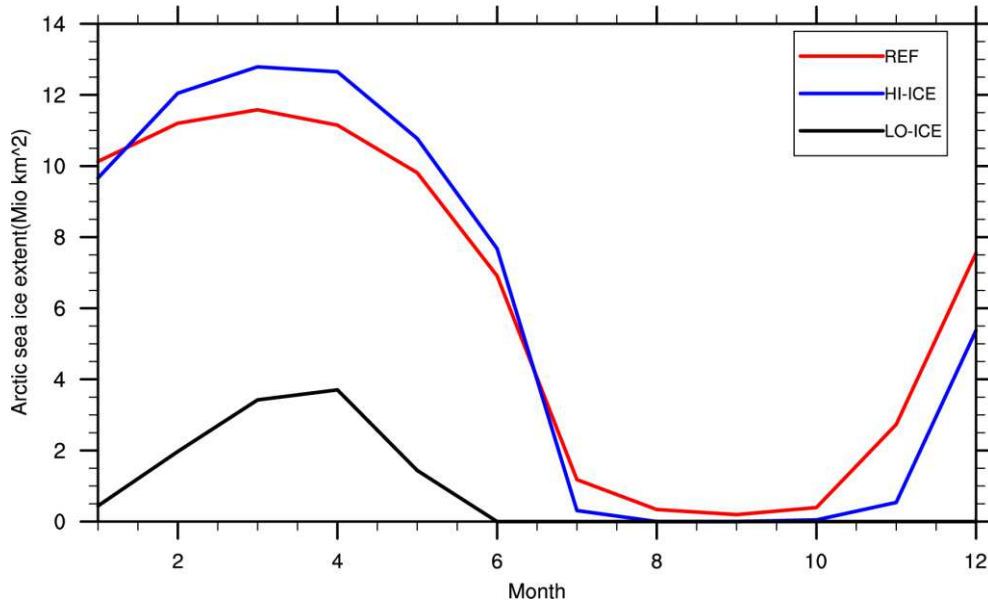


Figure 1 Annual cycle of sea ice cover averaged over North Hemisphere

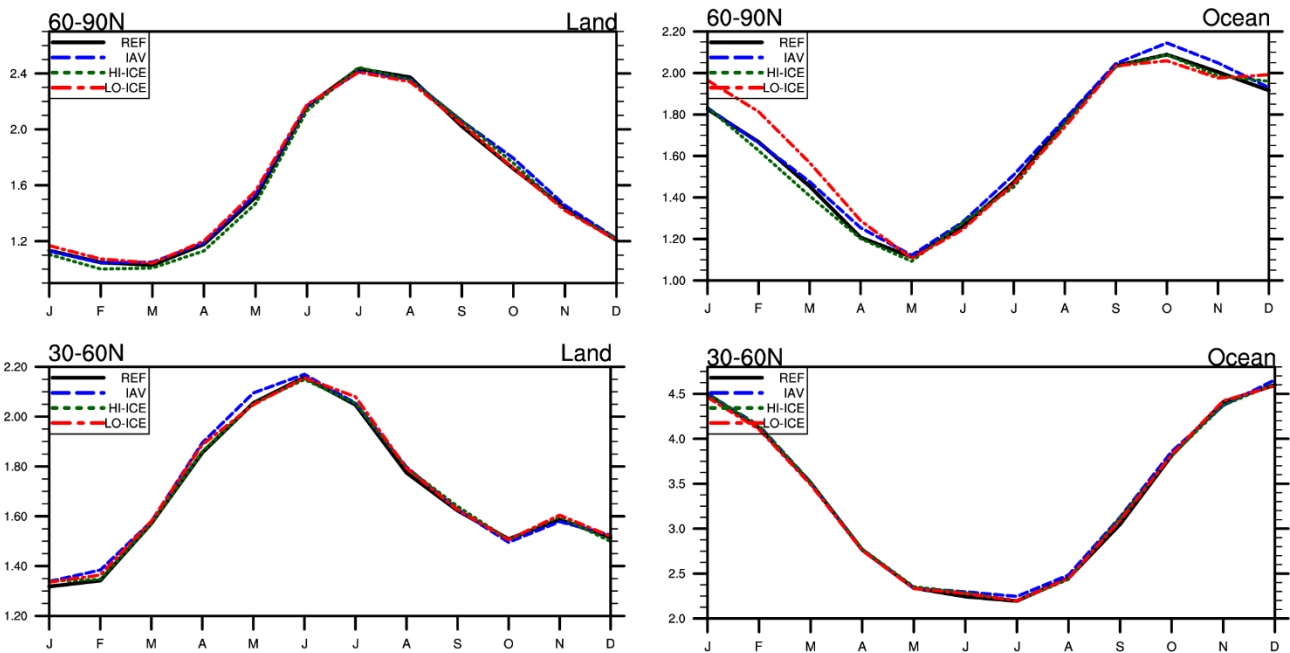


Figure 2 Annual cycle of precipitation averaged over the high-latitude(60°N-90°N) land and ocean, mid-latitude(30°N-60°N) land and ocean (unit: mm/day)

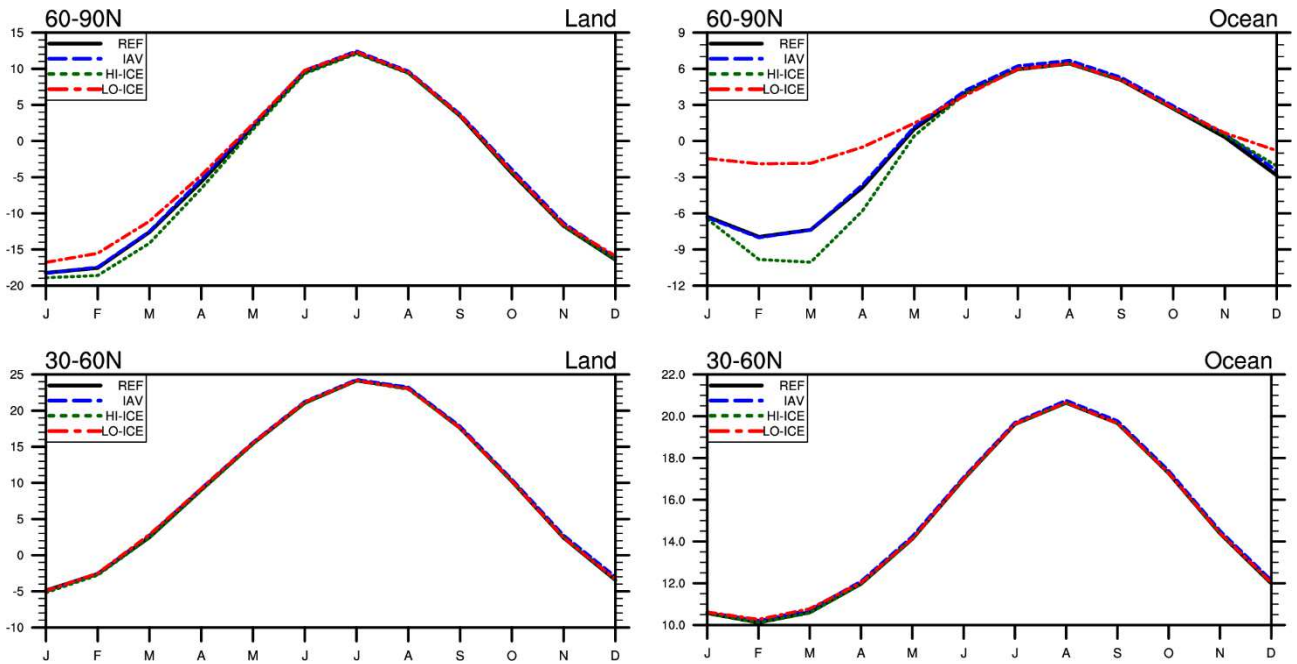


Figure 3 Annual cycle of Surface Air Temperature (SAT) averaged over the high-latitude(60°N-90°N) land and ocean, mid-latitude(30°N-60°N) land and ocean (unit: °C)

Surface Temperature

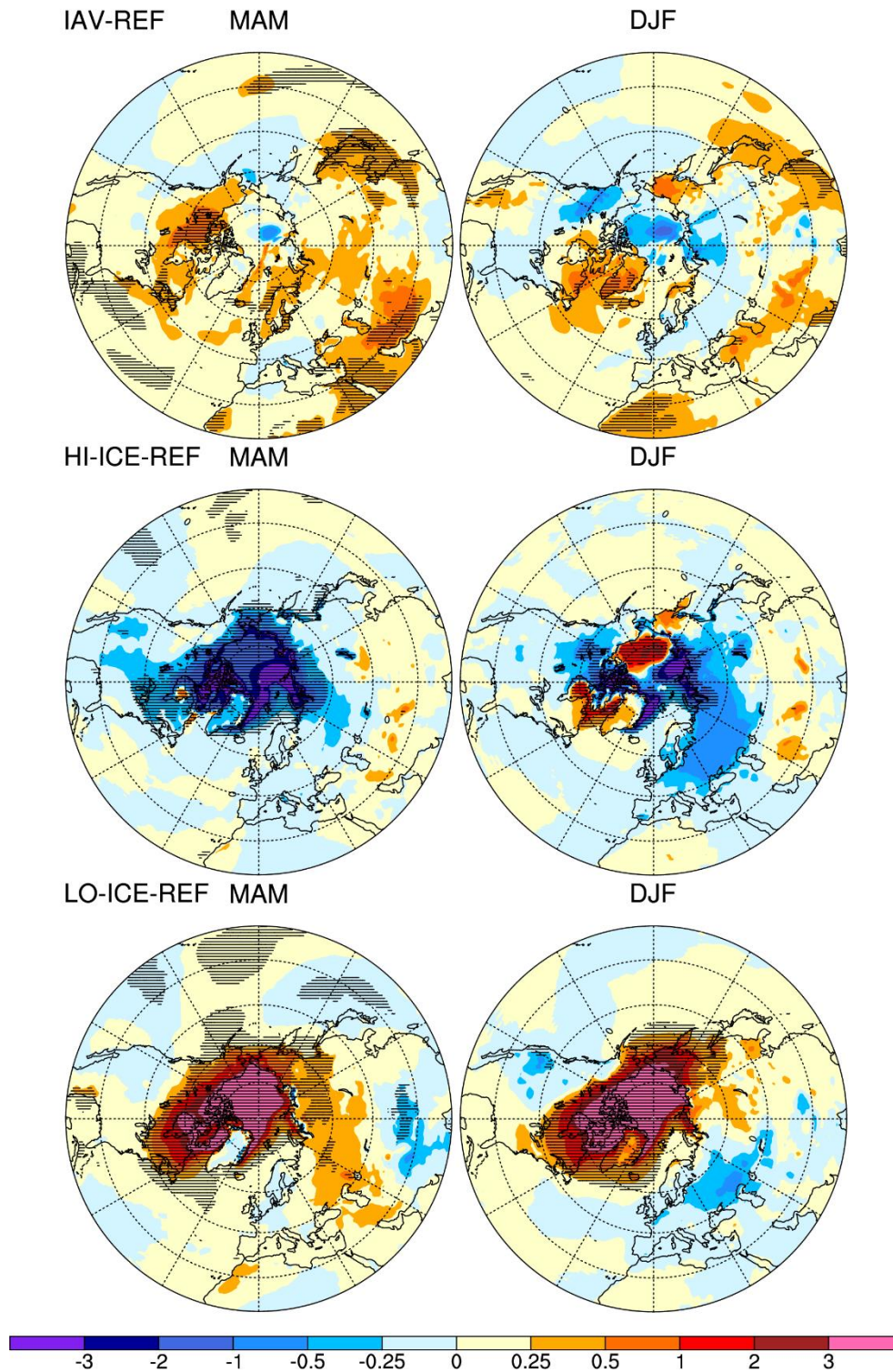


Figure 4 Surface Air Temperature (SAT) differences between experiments IAV, HI-ICE, LO-ICE and REF in Spring(MAM) and Winter(DJF) (Hatch area denotes significant values except 95% confidence level based on a Student's t-test) (unit: °C)

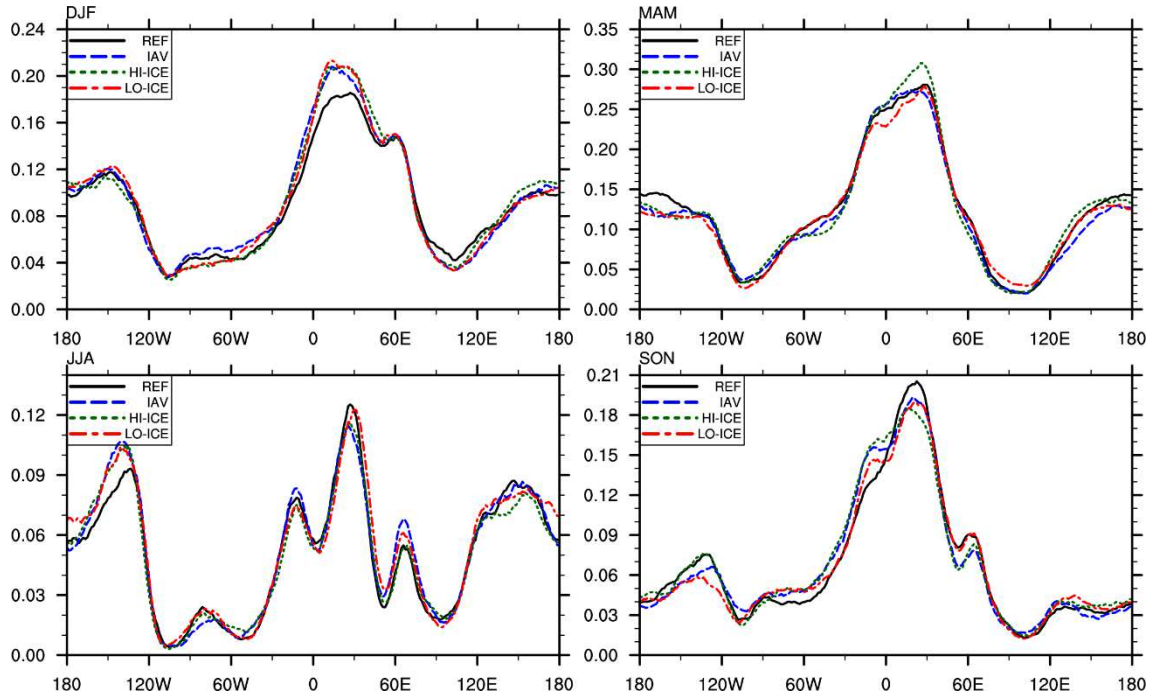
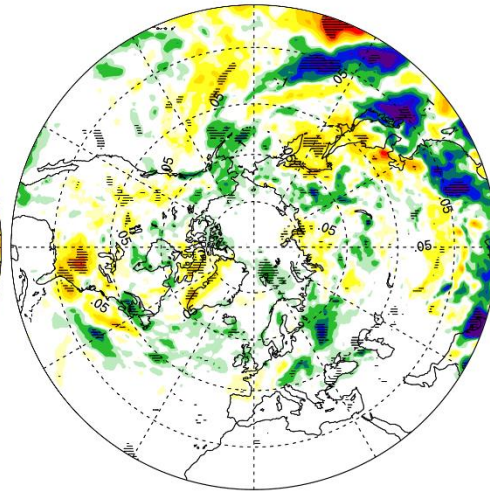
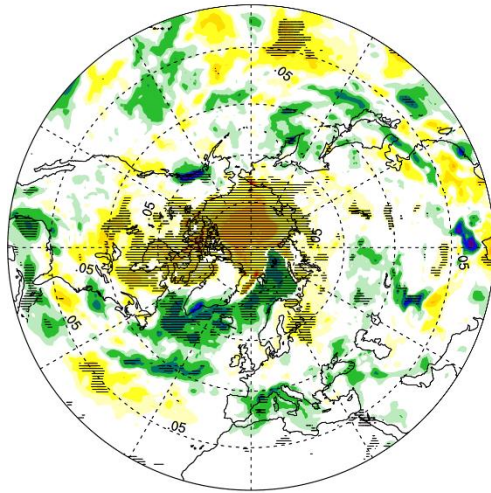


Figure 5 Seasonal blocking frequency for REF, IAV, HI-ICE and LO-ICE experiments (unit: %)

Precipitation

MAM

JJA



SON

DJF

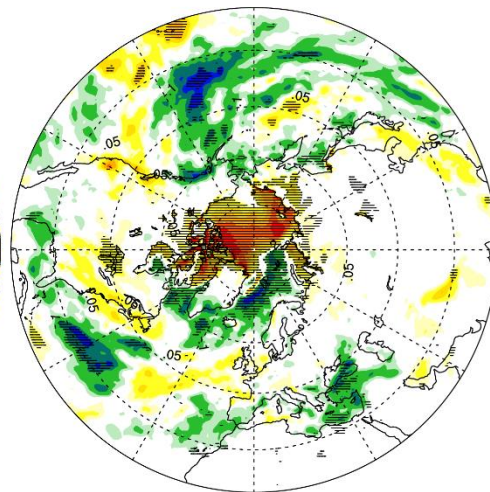
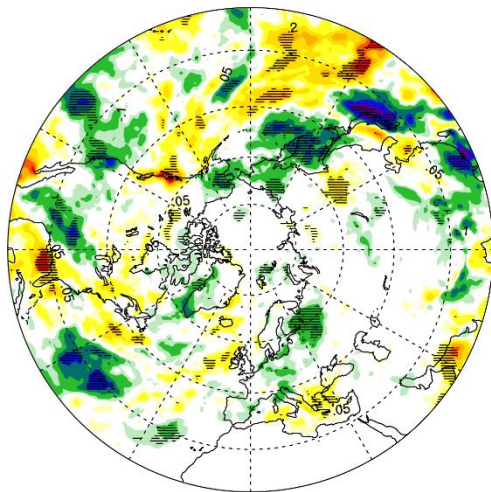


Figure 6 Precipitation differences between LO-ICE and HI-ICE experiments for MAM, JJA, SON and DJF (Hatched area denotes significant values except 95% confidence level based on a Student's t-test) (unit: mm/day)

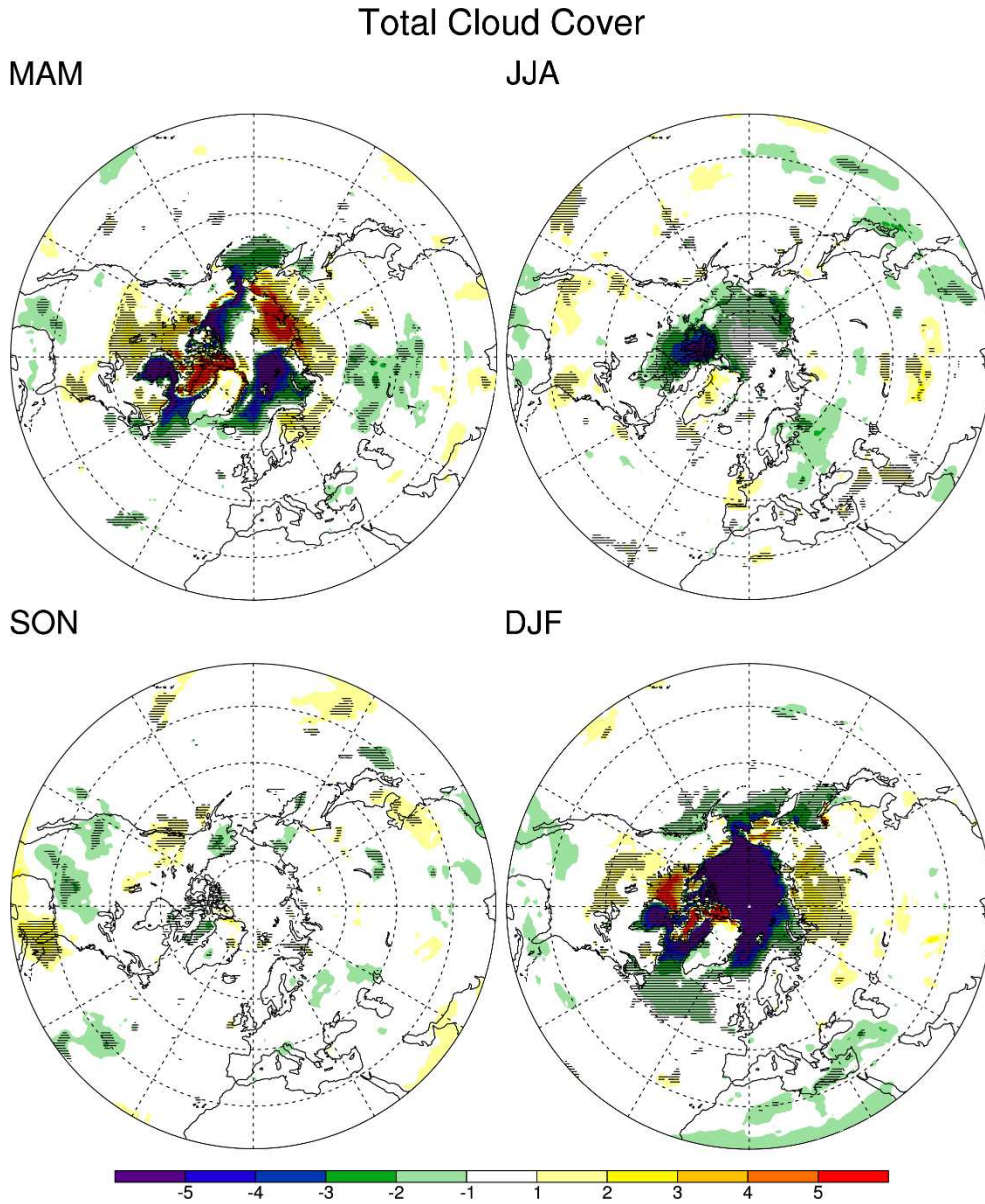


Figure 7 Total cloud cover differences between LO-ICE and HI-ICE experiments for MAM, JJA, SON and DJF (Hatch area denotes significant values except 95% confidence level based on a Student's t-test) (unit: %)

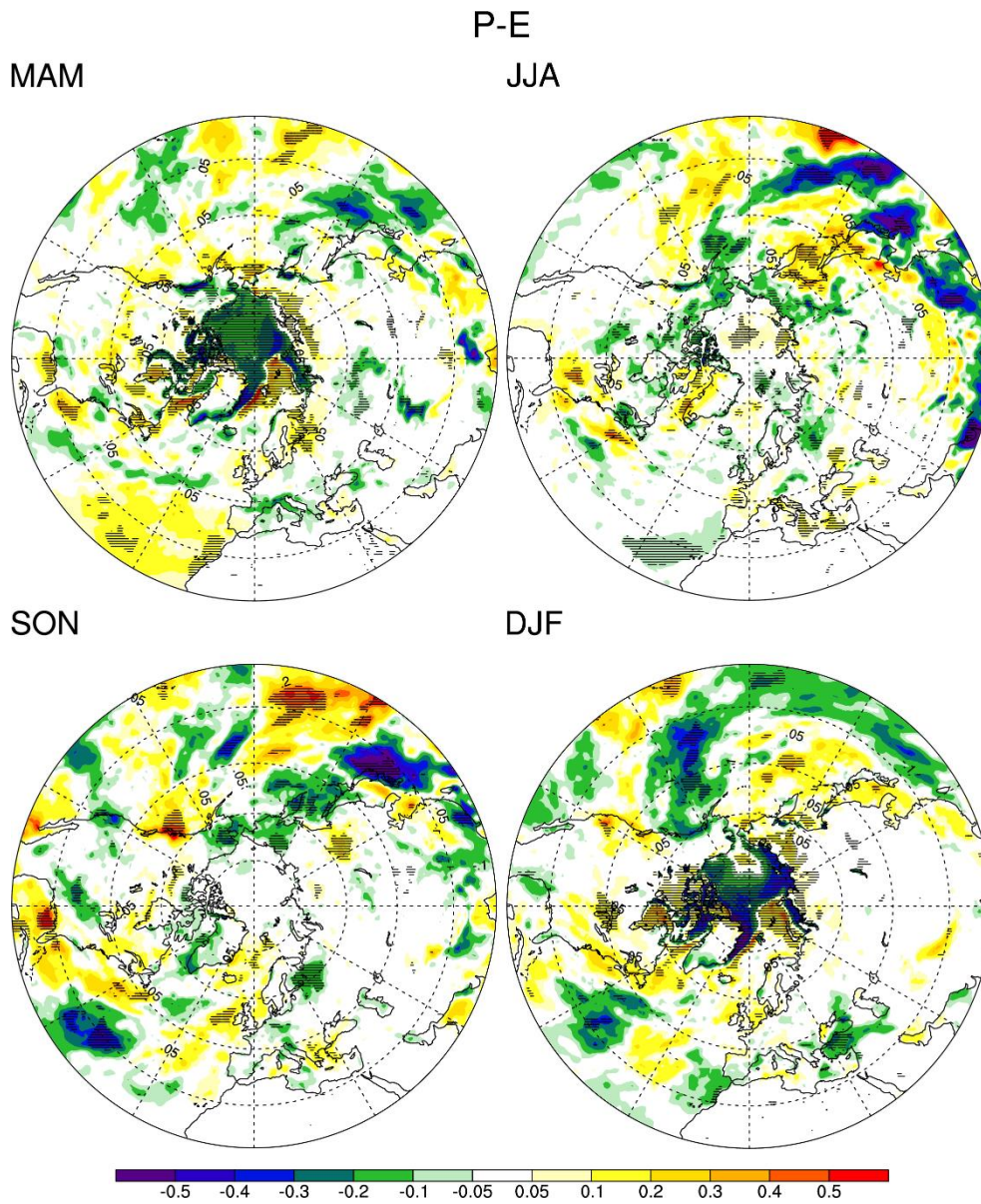
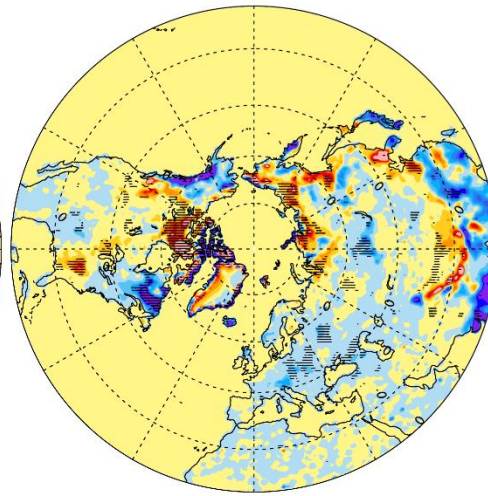
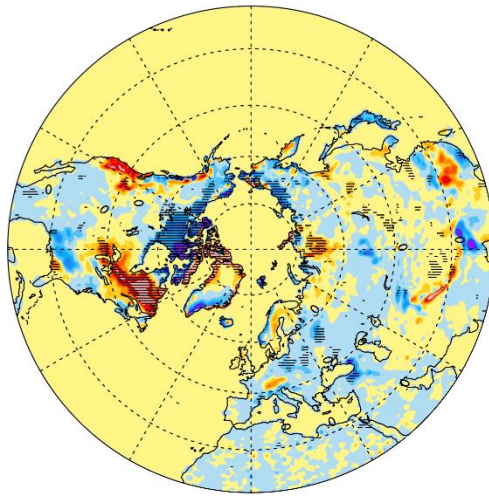


Figure 8 P-E(precipitation minus evaporation) differences between LO-ICE and HI-ICE experiments for MAM, JJA, SON and DJF (Hatch area denotes significant values except 95% confidence level based on a Student's t-test) (unit:mm/day)

Runoff

MAM

JJA



SON

DJF

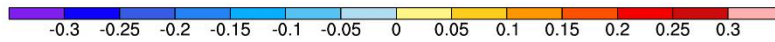
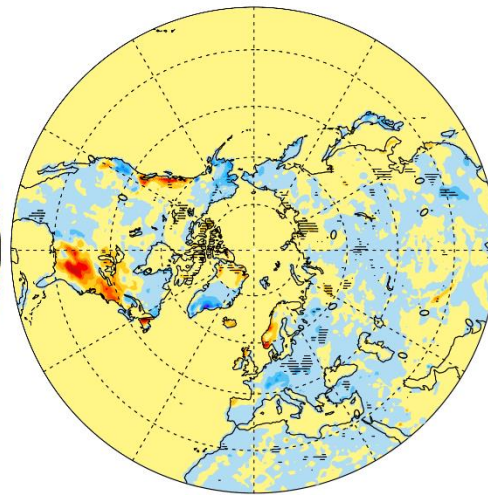
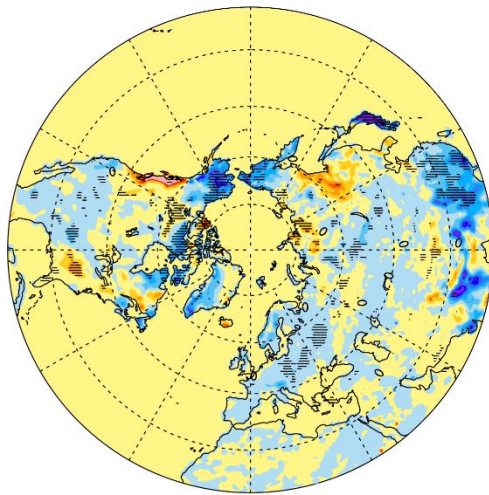
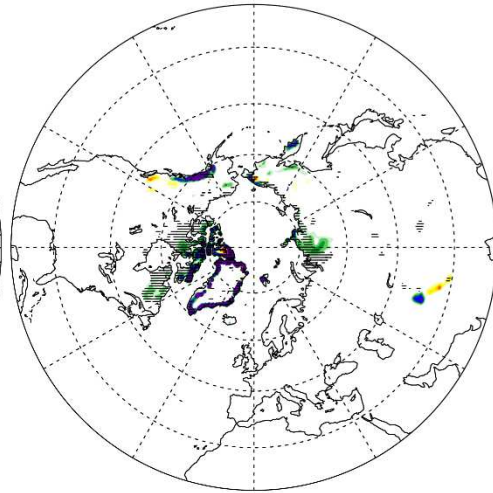
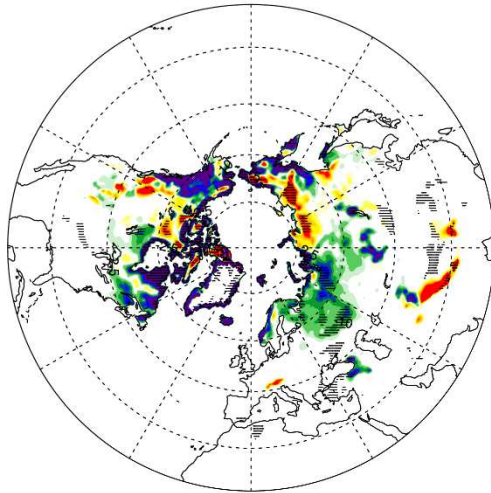


Figure 9 Runoff differences between LO-ICE and HI-ICE experiments for MAM, JJA, SON and DJF (Hatched area denotes significant values except 95% confidence level based on a Student's t-test)

Snow Depth

MAM

JJA



SON

DJF

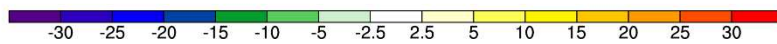
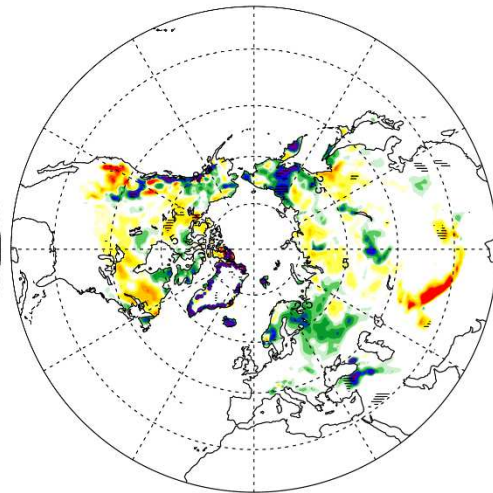
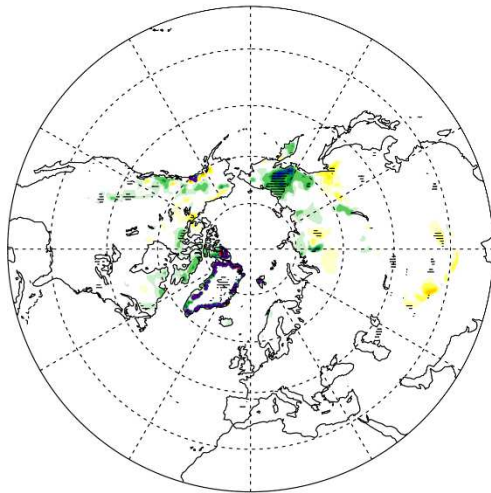
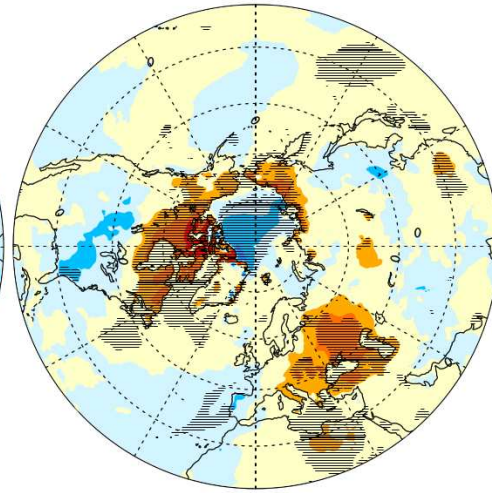
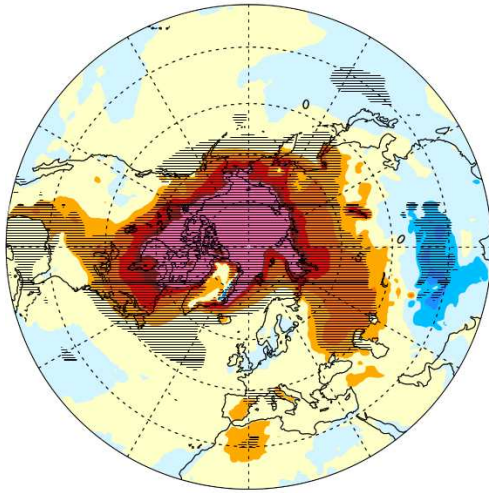


Figure 10 Snow depth differences between LO-ICE and HI-ICE experiments for MAM, JJA, SON and DJF (Hatched area denotes significant values except 95% confidence level based on a Student's t-test) (unit:mm)

Surface Temperature

MAM

JJA



SON

DJF

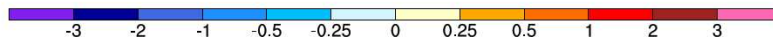
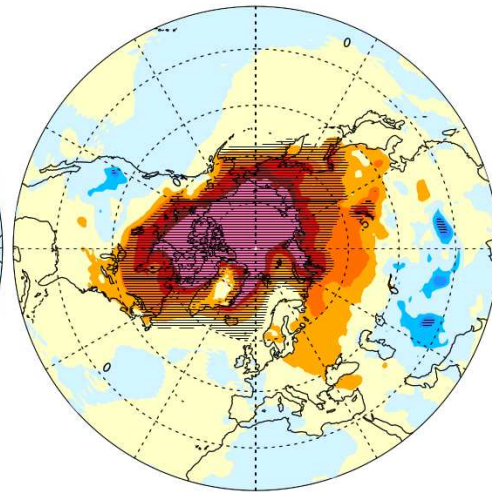
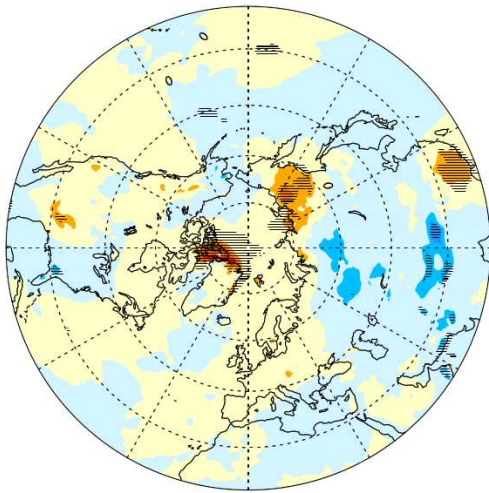
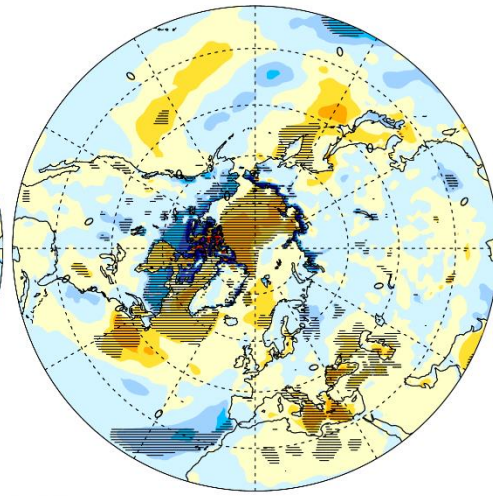
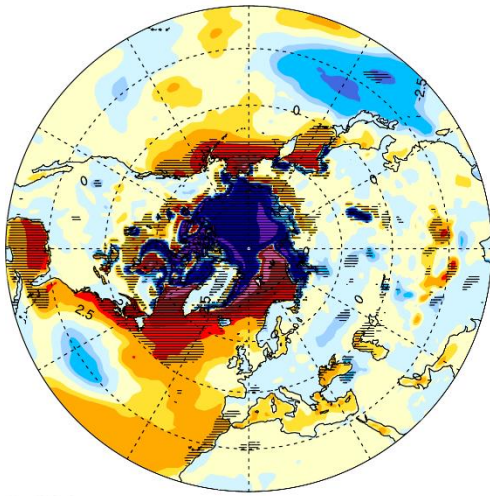


Figure 11 Surface Air Temperature (SAT) differences between LO-ICE and HI-ICE experiments for MAM, JJA, SON and DJF (Hatch area denotes significant values except 95% confidence level based on a Student's t-test) (unit: °C)

Turbulent Fluxes

MAM

JJA



SON

DJF

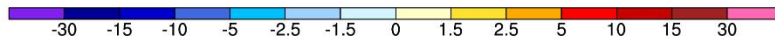
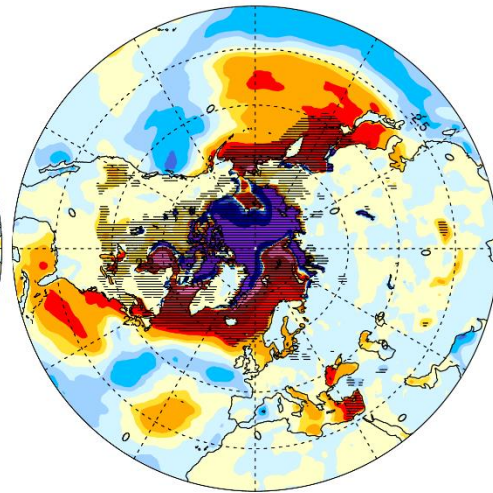
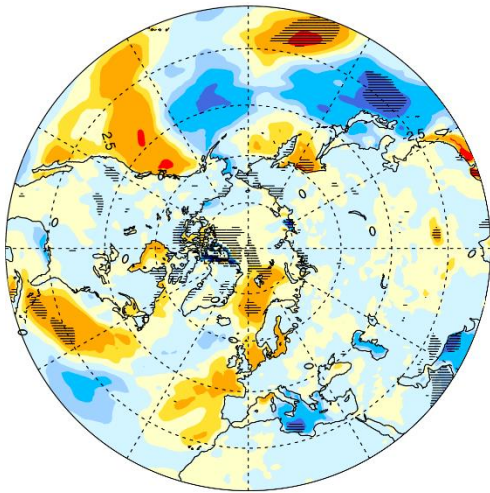
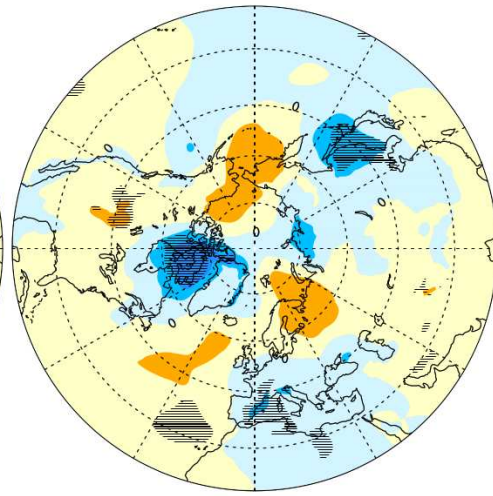
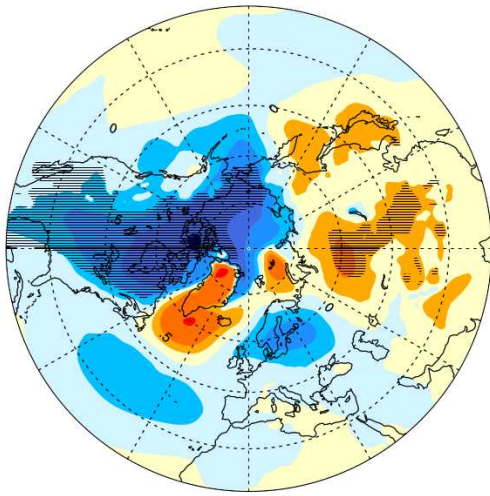


Figure 12 Turbulent fluxes(sensible heat flux + latent heat flux) differences between LO-ICE and HI-ICE experiments for MAM, JJA, SON and DJF (Hatch area denotes significant values except 95% confidence level based on a Student's t-test) (unit: w/m2)

Mean Sea Level Pressure

MAM

JJA



SON

DJF

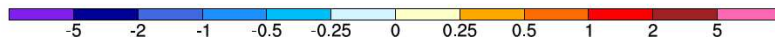
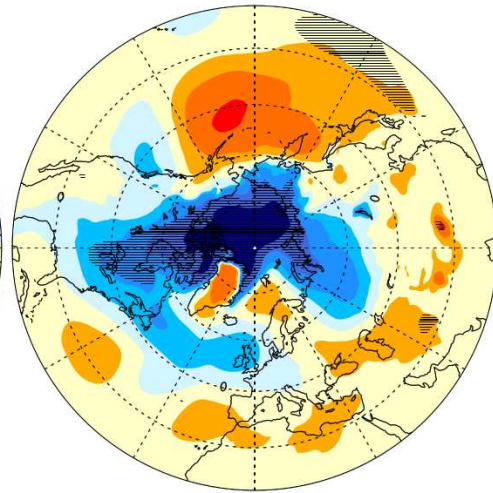
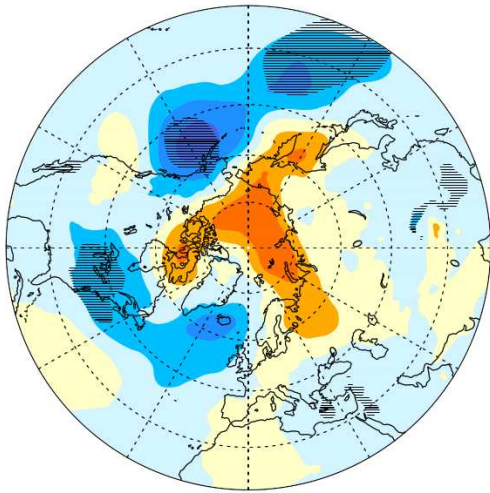
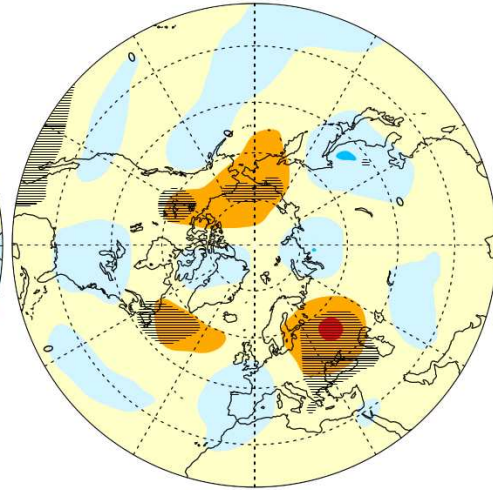
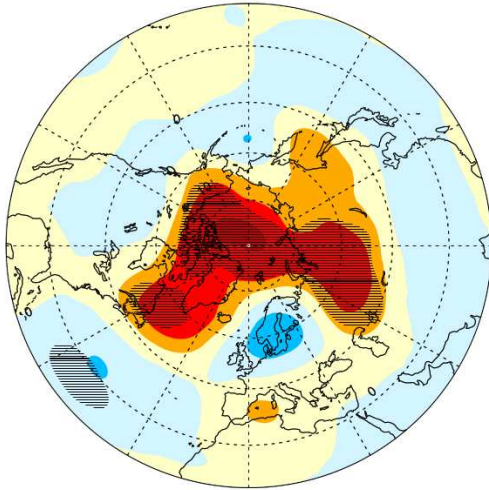


Figure 13 Sea Level Pressure (SLP) differences between LO-ICE and HI-ICE experiments for MAM, JJA, SON and DJF (Hatch area denotes significant values except 95% confidence level based on a Student's t-test) (unit: hPa)

500hPa Geopotential Height

MAM

JJA



SON

DJF

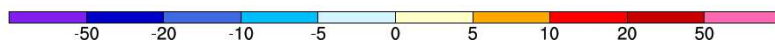
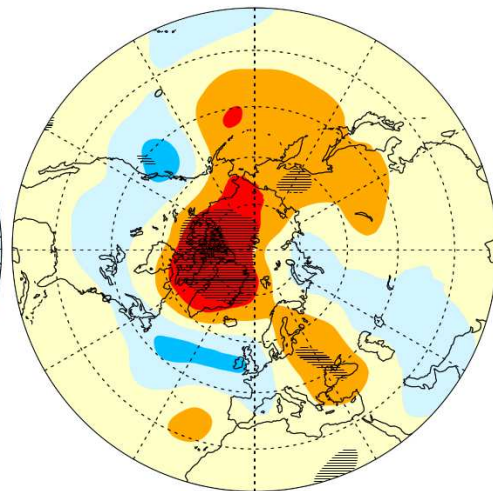
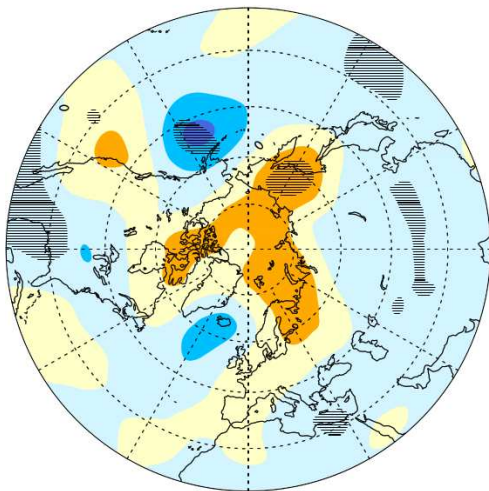


Figure 14 500hPa Geopotential Height differences between LO-ICE and HI-ICE experiments for MAM, JJA, SON and DJF (Hatch area denotes significant values except 95% confidence level based on a Student's t-test) (unit: meter)

Vertical Profile of Geopotential Height

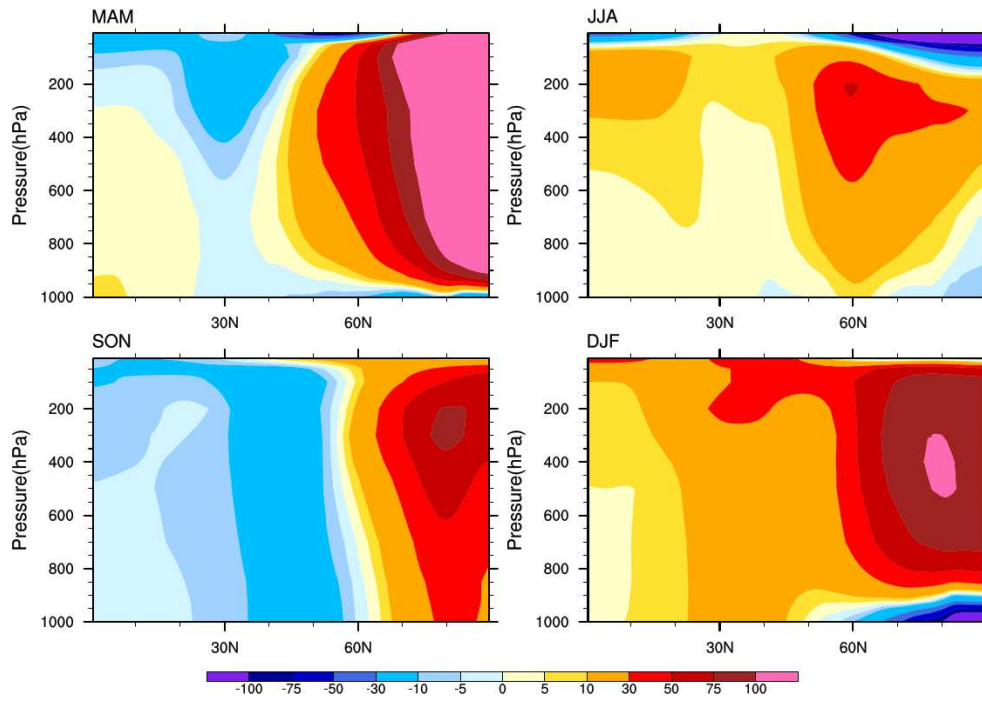
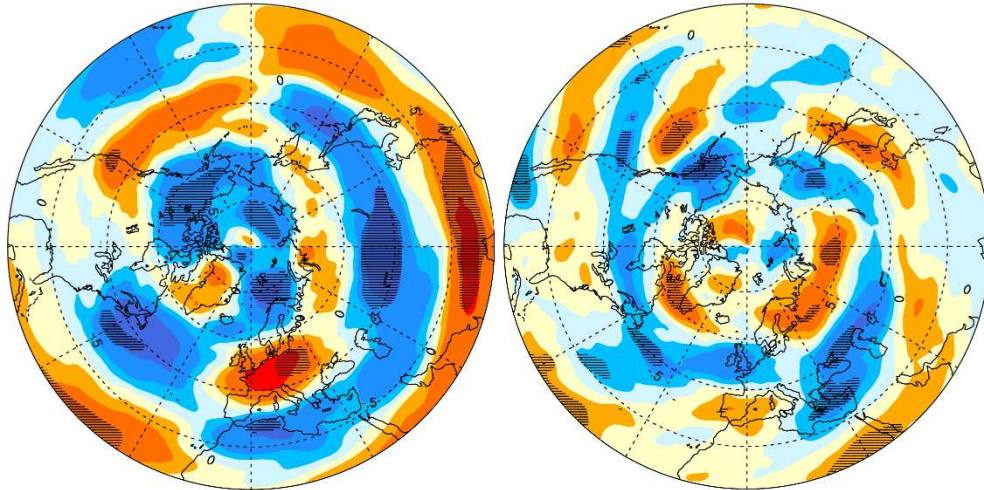


Figure 15 Vertical pattern of zonal-mean geopotential height differences between LO-ICE and HI-ICE experiments (unit: meter)

Zonal wind on 300hPa

MAM

JJA



SON

DJF

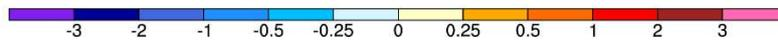
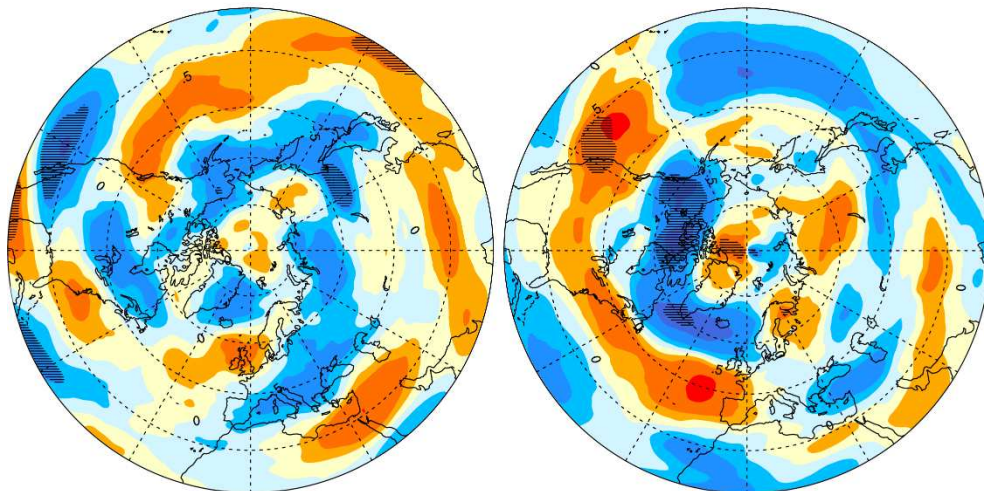


Figure 16 300hPa zonal wind differences between LO-ICE and HI-ICE experiments for MAM, JJA, SON and DJF (Hatch area denotes significant values except 95% confidence level based on a Student's t-test) (unit: m/s)

Vertical Profile of Zonal U

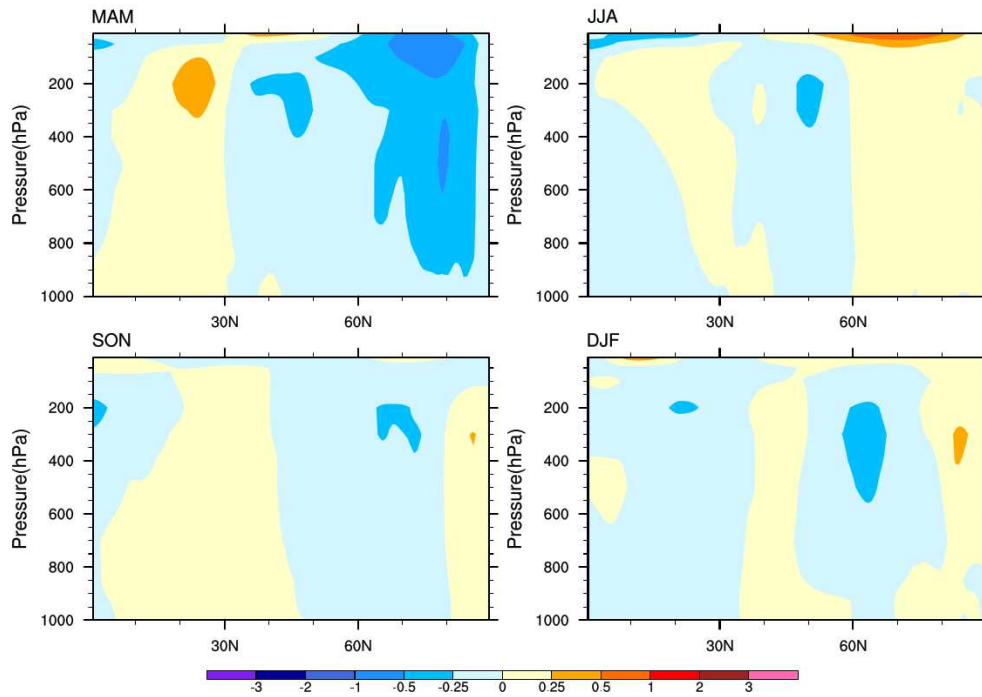


Figure 17 Vertical pattern of zonal-mean zonal wind differences between LO-ICE and HI-ICE experiments (unit: m/s)

Vertical Profile of Temperature

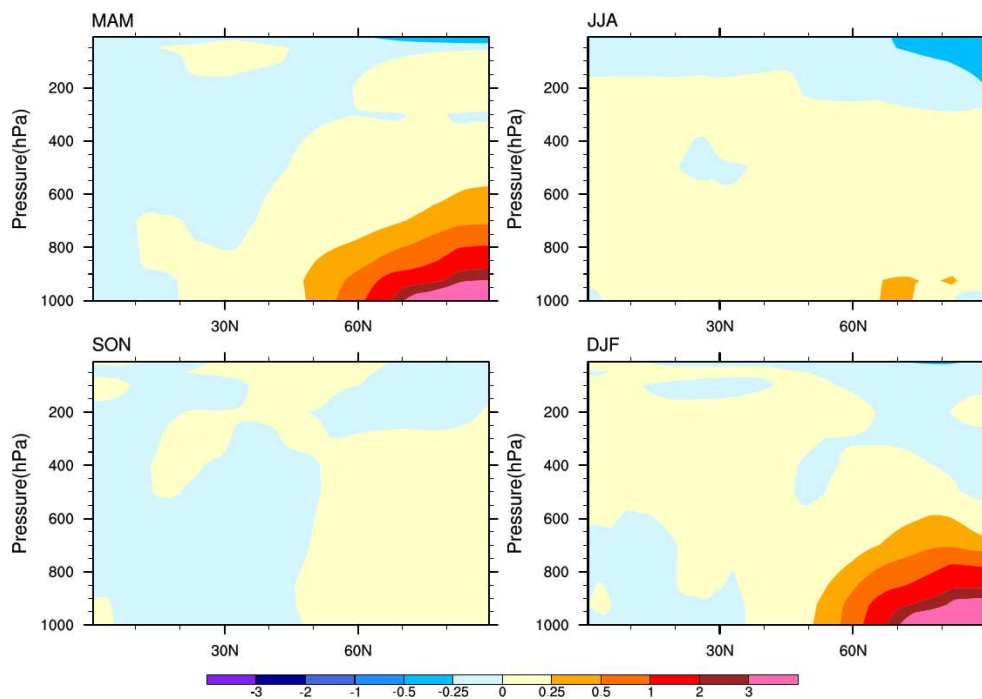


Figure 18 Vertical pattern of zonal-mean air temperature differences between LO-ICE and HI-ICE experiments (unit: °C)